# Genetically Encoded RNA Nanodevices for Cellular Imaging and Regulation

Qikun Yu,† Kewei Ren,† and Mingxu You\*

Department of Chemistry, University of Massachusetts, Amherst, Massachusetts 01003, USA

<sup>†</sup> These authors contributed equally

\* e-mail: mingxuyou@chem.umass.edu

## **Abstract**

Nucleic acid-based nanodevices have been widely used in the fields of biosensing and nanomedicine. Traditionally, the majority of these nanodevices were first constructed *in vitro* using synthetic DNA or RNA oligonucleotides and then delivered into cells. Nowadays, the emergence of genetically encoded RNA nanodevices have provided a promising alternative approach for intracellular analysis and regulation. These genetically encoded RNA-based nanodevices can be directly transcribed and continuously produced inside living cells. A variety of highly precise and programmable nanodevices have been constructed in this way during the last decade. In this review, we will summarize the recent advances in the design and function of these artificial genetically encoded RNA nanodevices. In particular, we will focus on their applications in regulating cellular gene expression, imaging, logic operation, structural biology, and optogenetics. We believe these versatile RNA-based nanodevices will be broadly used in the near future to probe and program the cells and other biological systems.

## 1. Introduction

Naturally existing DNAs and RNAs are polymer chains of nucleotides, which are comprised of only four bases: thymine/uracil, guanine, adenine, and cytosine. While, due to the diverse order of nucleotides, highly specific Watson-Crick base pairing, flexible design, and self-assembly property, nucleic acids have been widely used as a promising building material for various nanostructures and devices. In recent years, a diversity of two-dimensional or three-dimensional nucleic acid-based nanodevices have been constructed with unique features of structural programmability, spatial addressability, controllable length, size and shape, and easy synthesis and functionalization. These nanodevices, especially DNA-based ones, have been extensively applied in structural biology, bionanotechnology, *in vitro* diagnostics, cell membrane analysis, and nanomedicine. In the series of structural biology, bionanotechnology, *in vitro* diagnostics, cell membrane analysis, and nanomedicine.

Even though powerful, several concerns have been raised for the intracellular and *in vivo* applications of these nanodevices. For example, most majority of nucleic acid-based nanostructures and devices are *in vitro* prepared using chemically or enzymatically synthesized DNA/RNA oligonucleotides. For intracellular applications, these nanodevices have to be first delivered into cells. Even though several DNA nanodevices have been successfully developed for intracellular imaging, unfortunately, more general, highly efficient and non-invasive cellular delivery of nucleic acids is not always feasible.<sup>12–15</sup> Meanwhile, the enzymatic degradation of DNA/RNA, highly complex cellular environment, and potential cytotoxicity of synthetic compounds have made it even more challenging to apply artificial nucleic acid-based nanodevices for cellular studies.<sup>16,17</sup> In addition, the relatively low stability of large DNA nanostructures, e.g., DNA origami, at physiological Mg<sup>2+</sup> concentrations also restricts their applications inside cells.<sup>16</sup>

Compared with synthetic DNA nanodevices, functional RNA molecules can be genetically encoded and directly synthesized inside living cells using natural transcription machinery. A variety of RNA nanodevices exist in nature, including riboswitches, ribozymes, transfer RNAs, ribosomal RNAs, etc. These natural RNA devices play important roles in cellular functions by regulating metabolite recognition, RNA processing, and gene expression. Inspired by these natural RNA nanodevices, RNA nanotechnology have recently emerged to construct artificial functional devices for cellular imaging and regulation. Inspired by these natural RNA nanodevices can also be genetically encoded and continuously produced inside cells. The cellular expression of these nanodevices can be maintained at a constant level for a long period of time and across generations. The function of these RNA nanodevices can also be activated in either specific target cells or throughout the whole cell populations. As a result, these genetically encoded RNA devices provide an elegant solution to the problems with traditional synthetic nucleic acid-based tools in cellular deliveries and maintaining cellular concentrations and functions.

In this review, we will discuss the recent progress in the design, construction, and application of artificial genetically encoded RNA nanodevices. These artificial nanodevices can be rationally and programmably designed, providing a modular platform for intracellular applications. On one hand, by combining target-recognition functions with on-demand regulatory activities, artificial RNA nanodevices have been used for cellular gene regulation. On the other hand, genetically encoded RNA devices can also be applied as sensors for imaging and detecting various target analytes in living cells. More recently, even further advanced RNA nanodevices have emerged to regulate cellular protein and RNA networks, construct cellular logic circuits, and optogenetically

control RNA functions. By summarizing the design principles and features of existing RNA-based nanodevices, we hope this review will potentially inspire new structures and functions of these exciting molecular machines in the living systems.

## 2. Genetically encoded RNA nanodevices for gene regulation

In nature, both coding and non-coding RNAs play key roles in controlling cellular gene expression. At a last part of the service and sophisticated, which makes them hard to be modulated or altered for designable functions. Nowadays, artificially designed RNA nanodevices can also fold and react with protein partners to achieve gene regulation, but in contrast, the structure and function of these artificial RNA devices can be better predicted and controlled based on computational models, and various software are freely available online such as Mfold and NUPACK. At a last protein an important research area in synthetic biology. Compared with protein-based transcriptional and translational regulation, the use of RNAs has several advantages, including their easily predictable base-pairing interactions, dynamic binding-induced conformational changes, and the ability of systematically evolving new ligand-recognition unit, e.g., aptamers. To date, a couple of RNA-based designs have been developed into powerful gene regulation devices both *in vitro* and *in vivo*. At have been validated inside living cells for gene expression and regulation.

#### 2.1 Toehold reaction-based RNA nanodevices

One natural mechanism in achieving post-transcriptional gene regulation is by blocking the ribosomal access to the initiation site using either antisense small regulatory RNAs or mRNA-binding proteins.<sup>37</sup> Mimicking this natural regulation mechanism, the Collins group reported an artificial riboregulator device in 2004 that can either repress or activate translation in *Escherichia coli* (*E. coli*).<sup>38</sup> This engineered riboregulator consisted of two parts: a *cis*-repressed mRNA (crRNA) and a *trans*-activating RNA (taRNA) (Fig. 1a). The designed self-folding in the 5'-untranslated region of the crRNA kept the ribosome binding site (RBS) in a duplex formation and blocked it from recognizing the 30S ribosomal subunit. As a result, protein translation was inhibited. On the other hand, the taRNA was designed to hybridize with the stem and loop region in the crRNA. The resulting RNA duplex formation unfolded the crRNA, exposed the RBS region and permitted translation. A maximum of 19-fold increase in the GFP expression was observed in *E. coli* cells after activating the taRNA.<sup>38</sup>

Following this initial study, further optimized riboregulator with larger folds of gene activation and better ability of expressing multiple genes were demonstrated in *E. coli.*<sup>39</sup> Meanwhile, with minimal leakage, RNA riboregulator has been used to develop programmable kill switch for bacteria.<sup>40</sup> Based on a similar design principle, several other RNA riboregulators have been developed as well, which are again mostly tested within *E. coli* cells.<sup>41,42</sup> Even though these RNA riboregulators are able to regulate gene expression inside cells, these systems are still suffering from modest dynamic range, low specificity and orthogonality, and limited choice of sequences. The moderate dynamic range mainly stems from thermodynamically and kinetically unfavorable loop region-mediated interactions.<sup>43,44</sup> While limitations in sequence and low orthogonality come from the requirement of a double-stranded RBS region formation in the crRNA.

To overcome these challenges, an elegant RNA nanodevice was developed by the Yin group in 2014, which was named as toehold switches. These toehold switches consisted of a switch RNA and a trigger RNA (Fig. 1b). Unlike traditional RNA riboregulators, the RBS and start codon (AUG) regions in the switch RNA were completely unpaired, and as a result, the sequence of the trigger RNA is no longer constrained. Meanwhile, by replacing the "loop-loop" or "loop-linear" interactions with a toehold-mediated "linear-linear" interaction between unstructured RNAs, the accessibility of the trigger RNAs is also increased. With thermodynamically and kinetically more favorable toehold-mediated strand displacement reactions, these toehold switches can provide a much larger dynamic range (on average >400-fold) and better orthogonality in *E. coli* cells. These properties of toehold switches have already been comparable with those of optimized protein-based gene regulators. These toehold switches have been further integrated into bacterial genomes to regulate endogenous genes<sup>45</sup> and incorporated into cell-free paper-based platforms for *in vitro* diagnostics. More recently, toehold switches have also been engineered into various mammalian cell lines, including HEK293, HeLa and MDA-MB-231, for detecting microRNAs.<sup>47</sup>

Toehold reaction-based RNA nanodevices can not only regulate genes at the translational level, but also at the transcriptional level. 48,49 For example, the Lucks group created a small transcription activating RNA (STAR) nanodevice in 2015 to regulate bacterial transcription in *E. coli.* This STAR system composed of a transcription terminator-containing gene and a STAR antisense small RNA (Fig. 1c). Inspired by naturally existing pT181 transcriptional attenuator, an intrinsic terminator hairpin was designed to fold within the upstream of the regulated gene. The formation of this terminator caused RNA polymerase to terminate transcription before reaching the gene of interest. In the presence of the STAR antisense RNA, the terminator hairpin could be opened through toehold-mediated strand displacement reaction, which allowed the transcription elongation of the target gene. Based on this design principle, orthogonal pairs of STARs were developed with up to 94-fold gene activation. By further incorporating a computational design approach, highly efficient and orthogonal STARs have been engineered with maximally ~9,000-fold gene activation in *E. coli.* Similarly, toehold reaction-based RNA nanodevices can be used to transcriptionally inhibit bacterial gene expression as well. 49

## 2.2 Riboswitch- and Ribozyme-based RNA nanodevices

For decades, proteins have been considered as the only cellular component that could specifically recognize and response to small molecules. This observation was changed after the discovery of two kinds of natural RNA devices that can perform genetic regulation (i.e., riboswitches) or catalytic reactions (i.e., ribozymes). These naturally evolved RNA elements have been further engineered for specific gene regulation inside cells.

Since the first report of natural RNA riboswitches that can bind vitamin derivatives to regulate cellular vitamin synthesis in 2002,<sup>51–53</sup> plenty of riboswitches have been discovered in bacteria, archaea, plants, and fungi to recognize various target molecules including protein cofactors, nucleotides, amino acids, sugars, and ions.<sup>18,56,57</sup> These RNA riboswitches are composed of two components: a target-sensing aptamer domain and an expression platform (Fig. 2a). The target binding to the aptamer domain induces a conformational change in the expression platform, leading to the regulation of downstream genes. RNA riboswitch-based gene regulation can be achieved at both translational and transcriptional level. In the case of translation control, target binding-

induced RNA structural changes is often coupled with the sequestering or release of the RBS region, similar as that of the toehold switches.<sup>45</sup> To regulate transcription, similar as the STAR design, natural transcriptional attenuators are normally required in the function of these RNA riboswitches.<sup>48</sup>

With the help of RNA riboswitches, a number of cellular targets, especially metabolites, can now be incorporated for gene regulation. However, for most majority of synthetic compounds and many cellular components, natural RNA riboswitch partners have not yet been identified. These compounds, especially the synthetic ones, can be potentially highly useful in generating bioorthogonal gene regulation units in synthetic biology.

To identify specific RNA sequences for "any" given target molecule, Systematic Evolution of Ligands by EXponential enrichment (SELEX) is often used for the *in vitro* selection of RNA aptamers. <sup>58,59</sup> Like natural RNA riboswitches, some of these *in vitro*-identified RNA aptamers can also undergo conformational changes after binding with the target. As a result, these synthetic aptamers can be similarly placed in the 5' untranslated region of an mRNA to regulate genes. Interestingly, the initial successful attempt of these synthetic aptamer-based nanodevices was actually achieved in 1998 even before the discovery of natural RNA riboswitches. <sup>60</sup> In this case, aptamers that target Hoechst dyes were used to downregulate gene expression in Chinese hamster ovary cells. Similarly, the ability of *in vitro*-selected tetracycline and neomycin aptamers in gene regulation was also proved in yeast. <sup>61,62</sup> Besides these, synthetic theophylline-targeting RNA riboswitch is one of the most widely used RNA nanodevice for intracellular gene regulation. This is because theophylline exhibits great cell permeability and bioorthogonality, in addition, the corresponding aptamer can recognize theophylline with good specificity and binding affinity. After binding with theophylline, a predictable RNA conformational change is induced as a result. <sup>63–66</sup>

Even though a series of success have been achieved using synthetic RNA aptamers generated through *in vitro* SELEX, concerns over the *in vivo* selectivity and folding patterns of these nanodevices have influenced the broad usage of this new gene regulation platform. To overcome this challenge, several attempts have been made based on directed mutagenesis to reengineer natural RNA riboswitches for the binding of non-natural target ligands. These reengineered synthetic riboswitches were proved to function orthogonally to their original targets, which provided a promising alternative approach to regulate intracellular genes.

With increasing need of reliable and predictable nanodevices for gene regulation, another type of natural functional RNA molecules, ribozymes, have also become popularly used in engineering synthetic RNA devices. Natural RNA ribozymes are mostly involved in the catalytic processing of intron excision.<sup>57</sup> By fusing riboswitches or *in vitro* selected RNA aptamers with these ribozyme molecules, the resulting RNA nanodevices, termed ribozyme switches or aptazymes, are able to regulate gene expression in the presence of cognate target ligands (Fig. 2b). The most commonly used ribozyme for this purpose is the hammerhead ribozyme, which can perform *cis*- or *trans*-RNA cleavage once a three-way-junction catalytic core structure is formed.<sup>70</sup> Aptamers are normally fused into one stem junction of the hammerhead ribozyme. In the absence of the target, this stem region is unfolded, resulting in minimal cleavage. The target binding to the aptamer region induces the formation of the three-way-junction catalytic core and activates the ribozyme cleavage around the RBS region. It will then lead to the regulated protein translation. Using this design principle, hammerhead ribozyme-based RNA nanodevices have been activated inside cells using various

target molecules such as thiamine pyrophosphate,<sup>71</sup> theophylline,<sup>72–74</sup> tetracycline,<sup>75</sup> etc. In addition to the hammerhead ribozyme, other types of ribozymes, e.g., the twister ribozyme, could also be similarly used for gene regulation.<sup>76</sup> The catalytic function of these ribozymes have been used to improve the sensitivity of RNA nanodevices, while in the meantime, background signal leakage from spontaneous RNA cleavage has to be carefully optimized to achieve a large fold of gene activation/inhibition.

#### 2.3 CRISPR-based RNA nanodevices

Clustered regularly interspaced short palindromic repeats (CRISPR), together with CRISPR-associated protein (Cas), is one of the most powerful system for genetic manipulation.<sup>77</sup> On the basis of a simple RNA-guided sequence-specific DNA recognition, the CRISPR-Cas system is highly programmable and efficient.<sup>78</sup> With the help of engineered Cas9 protein and small guide RNA (sgRNA), targeted gene editing have been successfully demonstrated in various prokaryotic and eukaryotic cells, tissues, and animals.<sup>79–84</sup> In addition, without endonuclease activity, the catalytically dead Cas9 (dCas9) protein can also exhibit similar RNA-guided gene targeting property, which is useful for the reversible and inducible gene regulation.

Indeed, by designing synthetic RNA nanodevices to regulate sgRNA structures and functions, highly efficient and modular control of the CRISPR-Cas9 and CRISPR-dCas9 systems have been achieved. One success in using dCas9/sgRNA for the sequence-specific control of gene regulation, named CRISPR interference (CRISPRi), was achieved by Qi et al in 2013.<sup>85</sup> Because dCas9 is catalytically inactive, the dCas9/sgRNA complex would continue binding with their cognate DNA region and sterically block the transcription (Fig. 3a). CRISPRi can repress the target gene with up to 1,000-fold efficiency in *E. coli* cells.<sup>85,86</sup> By adding several different sgRNA sequences simultaneously, CRISPRi can be also used to regulate multiple genes. In addition, by coupling a transcriptional activator with dCas9, CRISPRi can also facilitate target gene activation.<sup>87</sup>

The above-mentioned toehold switches, riboswitch- and ribozyme-based nanodevices can also be introduced into the CRISPRi system to allow gene regulation by different RNA or small molecule triggers. For example, an inducible CRISPRi system was developed in 2016 by the Cai and Huang groups. In their design, a tetracycline-binding aptamer was inserted into the 3' end of the sgRNA. The stem region of the aptamer was designed to hybridize with the guide sequence of the sgRNA to inhibit its binding to the target DNA (Fig. 3b). The addition of tetracycline refolded the sgRNA and leaded to the desired binding and regulation of the target gene, as demonstrated in the HEK293T cells. By replacing the tetracycline-binding aptamer with other aptamer sequences, such as a theophylline-binding aptamer, different small molecules can also be used to regulate the efficiency of CRISPR-based gene regulation.

These target-binding aptamers can also be inserted in the middle of the sgRNA to achieve more versatile small molecule-controlled CRISPRi.<sup>89</sup> Theophylline- and 3-methylxanthine-binding aptamers have been used to demonstrate the function of these nanodevices for bacterial gene regulation. In another design, the Liu group have engineered a ribozyme-controlled sgRNA by linking a guanine-targeting aptazyme to the 5' end of the sgRNA (Fig. 3c).<sup>90</sup> The binding of guanine induced the cleavage of the ribozyme and activated the sgRNA for the cognate DNA recognition in the HEK293T cells. While it's worth mentioning that the self-cleavage of ribozyme could lead to some signal leakage in this system.

Besides small molecule-based triggers, nucleic acids can also be used to control the structure of the sgRNA. For example, conditional activation of the sgRNA can be achieved with the addition of a toehold sequence in its 5' end, which sequence will also block these DNA-recognition domains in both bacterial and mammalian cells. 91–93 In the presence of another trigger RNA, the sgRNA sequence can be released for targeted gene regulation. Another rational design strategy of inducible sgRNA was achieved by the Fulga group through the incorporation of a natural RNA-cleaving unit, such as endoribonuclease targeting region or antisense oligonucleotide-mediated RNase H cleavage site. 94 A modular and rapid control of the CRISPR functions was demonstrated based on this design. Indeed, these synthetic RNA nanodevices have provided an attractive and versatility approach in regulating CRISPR-based genetic modification.

## 3. Genetically encoded RNA nanodevices for intracellular imaging

## 3.1 Fluorogenic RNA aptamer-based imaging tags

In addition to regulate gene expression, another promising application of genetically encoded RNA nanodevices is for cellular imaging and detection of various target analytes. Traditionally, fluorescent protein (FP)-based reporters have been commonly used to construct protein- or RNA-based sensors for intracellular imaging. For example, based on the specific binding between an MS2 RNA hairpin and MS2 bacteriophage coat protein, RNA targets that are tagged with multiple copies of MS2 RNA can be imaged in living cells with FP-fused MS2-binding proteins. FP-based RNA nanodevices have also been developed to real-time monitor target analytes in living systems. However, there are still several challenges in applying these FP reporter-based RNA nanodevices. First of all, the large molecular weight of FP may interfere with the location and cellular functions of the nanodevice and target analytes. In addition, the limited choice of orthogonal RNA-protein binding pairs make it difficult for multiplex or programmable detection. Moreover, the high background fluorescence and limited dynamic range of existing FP-based RNA nanodevices have further prevented their wide applications.

Compared with FP-based reporters, it is more convenient and desirable to have genetically encoded RNA-based fluorescent reporters for these RNA nanodevices. Indeed as a result, fluorogenic RNA aptamers have been evolved. These RNA aptamers can selectively bind to small molecule chromophores and activate a corresponding fluorescence signal. A number of fluorogenic RNA aptamer/chromophore pairs with different spectral and biophysical properties have been developed recently, including so-called Spinach, Mango, Mango, Mango, Mango, Corn, Pepper, DNB, SRB-2108, etc (Table 1 and Fig. 4). With high signal-to-background ratio, easy programmability, and small size, these fluorogenic RNA aptamers have started being used as a versatile reporting unit in genetically encoded RNA nanodevices for intracellular imaging.

First of all, these fluorogenic RNA aptamers can be directly used as fusion tags for the imaging and tracking of cellular RNAs of interest. One fluorogenic RNA applied for this purpose was developed in the Jaffrey Lab in 2011 and was named as Spinach. Spinach can activate the fluorescence of a 3,5-difluoro-4-hydroxybenzylidene imidazolinone (DFHBI) chromophore. Several Spinach derivatives, such as Spinach2, Baby Spinach, and Broccoli, have been further developed with reduced size, improved brightness and folding capability. More recently, imaging of single

cellular RNAs have been achieved by using a tandem array of exceptionally bright fluorogenic RNA aptamer/chromophore pairs including Mango II/TO1-B, <sup>111</sup> Pepper/HBC, <sup>106</sup> Riboglow/ATTO590, <sup>112</sup> and Broccoli/BI. <sup>113</sup> Meanwhile, a wide spectral range ( $\lambda_{ex}$ , ~380–650 nm;  $\lambda_{em}$ , ~420–660 nm) of fluorogenic RNA tags are now available for various imaging purposes (Table 1 and Fig. 4).

Instead of using chemical chromophores, fully genetically encoded fluorogenic RNA system have also been developed based on RNA aptamers that can stabilize and activate FP fluorescence. Here, a bifunctional tDeg peptide, which can promote protein degradation, is fused to the C-terminus of fluorescent proteins. In the presence of an RNA aptamer, the tDeg peptide can bind with the aptamer and inhibit the proteasome-mediated FP degradation. As a result, a fluorescence signal can be generated. By adding ten concatenated RNA tags to a target mRNA, single mRNA molecule can also be imaged in living cells. 114

Besides functioning as a fusion tag, fluorogenic RNA aptamers have also been used to construct various interesting dynamic RNA nanodevices for cellular target detection and imaging. In these nanodevices, generally, the fluorogenic RNA aptamers are designed to be unfolded initially, resulting in an off-state with low background fluorescence signal. Once the target is present, a conformational change in the RNA nanodevice is induced to re-fold the fluorogenic RNA aptamers and further activate the fluorescence signal. As a result, these fluorogenic RNA-based nanodevices can be used to detect a wide variety of analytes of interest. In the following sections, we will discuss the design principles and applications of these smart RNA sensors.

## 3.2 Split fluorogenic RNA aptamer-based nanodevices

One design strategy to regulate the formation of fluorogenic RNA aptamers is based on the split version of these aptamers. By dividing fluorogenic RNA aptamers into two separate fragments, the chromophores cannot bind with the aptamers and thus exhibit minimal background fluorescence signal. The target analyte is normally designed to bind with both fragments of the split aptamer and bring them into proximity. As a result, fluorogenic RNA aptamers can be reassembled to activate the fluorescence of chromophores.

For example, based on a split version of Broccoli, the Fan group have developed an aptamer-initiated fluorescence complementation method for imaging endogenous RNAs in living mammalian cells, including HeLa and human umbilical mesenchymal stem cells (HuMSC). Here, each fragment of the split Broccoli was appended with a sequence complementary to the target mRNA. The target hybridization will then induce the formation of an active DFHBI-binding site, as well as the fluorescence activation (Fig. 5a). By replacing the target recognition sequences, these split RNA aptamer-based nanodevices can be easily designed and extended for imaging different endogenous RNA targets. As another example, the Burke group have recently applied a similar split-Broccoli system to monitor intracellular RNA-RNA interactions in *E. coli* cells. Only when two RNA strands bind with each other, the fluorescence signal of the cognate fluorophore can be activated.

These split fluorogenic RNA aptamers can also be used to improve the sensitivity of RNA-based nanodevices. For example, our group have developed a fluorogenic RNA-based genetically encoded RNA circuit in 2018, termed CHARGE, by combining a catalytic hairpin assembly (CHA) system with split Broccoli (Fig. 5b).<sup>117</sup> CHA is an efficient enzyme-free amplification system based

on the target-induced catalytic hybridization of two hairpin structures. By conjugating split Broccoli fragments, respectively, to the terminal of these two hairpins, the target RNA-induced CHA activation will lead to the reassembly of the Broccoli structure and activate the DFHBI fluorescence. One target can catalytically generate tens-to-hundreds of Broccoli, and as a result, the CHARGE circuit can be used to image RNA targets in living *E. coli* cells with very high sensitivity.

One potential limitation of the CHARGE device is that it cannot be used to track the subcellular location and distribution of the targets. To solve this problem, we have also engineered another split Broccoli-based circuit, which was named as an IN Sltu Genetic Hybridization Amplification Technique (INSIGHT). INSIGHT functions based on a hybridization chain reaction between a pair of split Broccoli-modified hairpins. Once a target RNA is generated inside cells, a cascaded hybridization of these two hairpins will be triggered to generate a chain of Broccoli (Fig. 5c). Because the generated Broccoli chain will directly bind with the target RNA, the INSIGHT system can be used to image the distribution and cellular location of the target analytes in both bacterial and mammalian cells.

## 3.3 Allosteric fluorogenic RNA aptamer-based nanodevices

Another commonly used design strategy of fluorogenic RNA-based sensors is based on the target-induced allosteric structure change of the RNA aptamers. In this design principle, a target-binding aptamer is directly connected to the fluorogenic RNA aptamer through a transducer RNA module (Fig. 6a). In the absence of the target, both the target-binding aptamer and fluorogenic RNA aptamer are unfolded. The binding of the target will then stabilize the transducer and refold the fluorogenic RNA aptamer, turning on the fluorescence. Using Spinach as the reporter, the Jaffrey group developed a type of allosteric fluorogenic RNA sensors in 2012 for imaging the cellular dynamics of adenosine 5'-diphosphate and S-adenosyl methionine in *E. coli* cells. <sup>121</sup> Based on a similar design, several allosteric Spinach-based sensors have been further developed for the intracellular imaging of various small molecules and proteins in bacterial cells, including cyclic di-AMP, <sup>122</sup> cyclic di-GMP, <sup>123</sup> cyclic AMP-GMP, <sup>123</sup> Streptavidin, <sup>124</sup> MCP coat protein, <sup>124</sup> etc. In addition to Spinach, other fluorogenic RNA aptamers, such as Broccoli and red Broccoli, have also been applied to construct allosteric sensors for imaging 5-hydroxy-L-tryptophan, <sup>125</sup> 3,4-dihydroxy-L-phenylalanine, <sup>125</sup> S-adenosyl methionine, <sup>126</sup> etc. in living bacterial and mammalian cells.

Although a number of allosteric fluorogenic RNA sensors have been developed to image cellular analytes, almost all of these sensors are developed based on a single RNA fluorescent reporter. Considering the variations in the cellular RNA expression and distribution, it is difficult to directly apply these single-color sensors to quantify target cellular concentrations. Our group have developed a ratiometric fluorogenic RNA device to solve this problem. Our ratiometric sensor contains two fluorogenic RNA aptamer/chromophore pairs, Broccoli/DFHBI and DNB/SR-DN (Fig. 6b). The Broccoli and DNB aptamers were connected *via* a three-way junction F30 scaffold. The DNB aptamer was further engineered into an allosteric sensor by fusing with a target-binding aptamer, while Broccoli was used as a reference unit to normalize the cell-to-cell variations in the RNA expression level. The DNB-to-Broccoli fluorescence ratio can then be applied for the quantitative imaging of adenine, tetracycline and c-di-GMP in bacterial cells. By replacing SR-DN with a more stable TMR-DN chromophore, these ratiometric allosteric RNA nanodevices can further monitor the dynamic variations in the target cellular concentrations. 128

### 3.4 Riboswitch- and ribozyme-based fluorogenic RNA nanodevices

As mentioned above, riboswitches are naturally evolved RNA nanodevices that can recognize various cellular targets and then exhibit conformational changes to modulate gene expression. <sup>18,22</sup> Compared with *in vitro*-identified aptamers, riboswitches are capable of providing more selective and precise response to the natural concentration changes of the target analytes. <sup>129</sup>

Inspired by the function of these natural riboswitches, we have previously constructed synthetic riboswitch-based RNA sensors to detect different cellular targets. For example, by replacing the gene expression platform of a natural riboswitch with Spinach, a so-called Spinach riboswitch nanodevice was designed for imaging metabolites in live bacterial cells (Fig. 7a). In the absence of the target, the transducer sequence in Spinach will hybridize with a switching sequence in the target-binding aptamer, resulting in a minimal fluorescence intensity. Target binding to the riboswitch will then release the transducer sequence and induce the folding of Spinach to capture DFHBI and activate its fluorescence signal. This design strategy has been exploited to develop a series of Spinach riboswitch nanodevices for the intracellular detection of thiamine pyrophosphate, guanine, adenine, and S-adenosyl methionine.<sup>130</sup>

Ribozymes are another type of functional RNA nanodevices that enable catalytic cleavage of RNA substrates at specific positions. Due to their easy design, predictable structure, and controllable activity, ribozymes have been used as a useful tool for constructing biosensors. By fusing target-binding aptamers with ribozymes, allosteric ribozyme sensors have been designed to detect different biomolecules. Based on these allosteric ribozymes and a Broccoli reporter, a type of RNA-based catalytic sensors, named RNA integrators, have been developed for low-abundance metabolite detection in living *E. coli* cells (Fig. 7b). In the presence of the target analyte, the folding of the target-binding aptamer would activate the ribozyme cleavage, which subsequently triggered the release of an inhibitory Broccoli sequence. As a result, the Broccoli aptamer was reassembled to activate the DFHBI fluorescence. Since each target molecule can bind and induce cleavage of multiple RNA integrators, the fluorescence signal could be amplified.

#### 3.5 Fluorogenic RNA aptamer-based FRET sensors

Another promising sensor design strategy is based on fluorescence resonance energy transfer (FRET). FRET is a non-radiative energy transfer process between an excited fluorescent donor and a ground-state acceptor. The FRET efficiency is highly dependent on the distance and orientation of the donor and acceptor fluorophores. FRET-based sensors have an inherent sensitivity to the environment and conformation changes, which provide a powerful approach for probing the temporal and spatial variations of target molecules and biological processes.

RNA nanodevices, with defined shape, size, and stoichiometry, have been constructed to precisely assemble different protein and RNA molecules. A very interesting RNA origami structure has been recently used to build a fluorogenic RNA aptamer-based FRET nanodevice in *E. coli* cells (Fig. 8). Using only a single-stranded RNA, this origami structure can be genetically encoded and used as a scaffold to position two fluorogenic RNA aptamers in different orientations and proximities. After optimizing the distance and relative dipole moment, the FRET signal between a Spinach and a Mango RNA aptamer was used for the detection of target RNAs and small molecules. Upon target binding, the conformation of the RNA origami was altered, which further changed the orientation and distance between Spinach and Mango, leading to changes in the FRET

outputs. Further optimized FRET-based RNA nanodevices can be potentially used for the quantitative and rapid imaging of various target analytes.

## 4. Genetically encoded RNA nanodevices for other cellular functions

## 4.1 Genetically encoded RNA nanodevices to perform cellular logic operations

Natural biological systems are always presenting in a complex environment that require a rapid sensing of multiple input signals, a logic analysis, and then an accurate output response. Inspired by the natural gene network, sophisticated DNA-based circuits have been engineered *in vitro* for information storage, computing, and diagnostics. While these DNA-based circuits are difficult to be used inside cells, genetically encoded RNA nanodevices have been created to perform intracellular logic operations with the goal of regulating cellular functions in a more precise way. 149

For example, by coupling both theophylline and TPP aptamers to the 5' untranslated region of a mRNA, the Yokobayashi group have previously engineered Boolean AND and NAND logic gates to control gene expression inside *E. coli* cells. Similarly, the Smolke group have developed another modular ribozyme-based RNA nanodevice to achieve theophylline- and tetracycline-mediated cellular logic AND, NOR, OR, and NAND operations. Most of these initial attempts of RNA-based logic devices function only with two input signals.

A significant improvement in the programmability of these RNA nanodevices was achieved based on the toehold switches.<sup>45</sup> After an initial demonstration of a four-input AND logic gate function inside *E. coli* cells, the further optimization of RNA sequences has led to the development of more complex logic network, for example a 12-input logic circuit, i.e., one of the most complicated synthetic logic expression system realized in living cell.<sup>152</sup> These toehold switch-based nanodevices can also be designed to repress bacterial gene translation with up to four inputs.<sup>153</sup>

Besides toehold switches, the above-mentioned STAR- and CRISPR-based nanodevices have also been validated to perform two- or three-input logic operations inside *E. coli* cells.<sup>50</sup> These and other genetically encoded RNA nanodevices have further expanded the toolbox of programmable computing units for constructing synthetic intracellular circuits and information network.

## 4.2 Genetically encoded RNA nanodevices for structural biology studies

DNA nanotechnology has been used to construct various highly precise nanostructures that can be used as *in vitro* scaffolds to arrange biological molecules in a specific pattern. These rationally designed DNA nanostructures have been further applied to study and regulate the functions and interactions of various target molecules. Interestingly, these DNA nanostructures can now also be genetically encoded through phagemid in bacterial cells. Compared with chemically synthesized DNA molecules, these intracellular DNA nanostructures can be cost-effectively produced, especially when a large amount of DNAs are needed. Even though these genetically encoded DNA nanostructures can be potentially useful in producing scalable nanodevices for *in vitro* applications, the limited adaptability of these phagemid-based expression system make it hard to directly apply these DNA nanodevices for cellular analysis or regulation.

In contrast, genetically encoded RNA nanostructures are believed to be more applicable because of

the single-stranded nature of cellular RNA molecules. In addition, natural RNA-protein interactions and non-Watson-Crick RNA interactions can also facilitate the construction of complex nanostructures inside living cells. The initial attempt of constructing synthetic genetically encoded RNA nanostructures was based on the self-assembly of short RNA modules. After transcription, these short RNA modules can hybridize with each other to construct one-dimensional or two-dimensional RNA structures. These structures have also been used as scaffolds to bind and spatially organize different proteins for the controlled chemical reactions inside bacterial cells.

More recently, the self-folding of a long RNA strand into a designed nanostructure has been achieved both *in vitro* and inside *E. coli* cells. <sup>162,164–166</sup> Compared with multicomponent assembly of short RNA modules, these self-folded single-stranded RNA nanostructures can be more rapidly folded and with higher yield. Indeed, the co-transcriptional folding of these nanostructures have been successfully demonstrated. This is a critical feature for reducing the potential degradation or misfolding of these RNA nanostructures during intracellular applications. These single-stranded RNA nanostructures have already begun to exhibit interesting cellular functions, for example, in the above-mentioned RNA origami-guided fluorogenic RNA FRET system. <sup>144</sup> With further optimized design and characterization strategy, these versatile self-assembled RNA nanostructures can be highly useful in future to spatially arrange different cellular components for structural biology studies and to regulate cellular interactions.

## 4.3 Genetically encoded photo-responsive RNA nanodevices

Using light to control cellular functions is always an attractive approach because of the high spatial and temporal resolution of light. The idea of using light to regulate the function of genetically encoded RNA nanodevices has been proposed for a while.<sup>21</sup> Several light-regulated RNA switches have been indeed demonstrated *in vitro* based on the specific recognition of RNA aptamers towards a particular photo-induced isomerization state of the chromophore.<sup>167,168</sup> Unfortunately the intracellular performance of these chromophore-mediated RNA nanodevices have not yet been validated.

Very recently, exciting photo-responsive RNA nanodevices have been engineered by the Mayer and Möglich groups to regulate cellular gene expression in HeLa cells. <sup>169</sup> In these nanodevices, an RNA aptamer, which can specifically recognize a bacterial light-oxygen-voltage photoreceptor (PAL) under blue light, was inserted into the 5' untranslated region of a gene reporter. After the PAL-RNA conjugation, the gene expression can be sterically inhibited in both bacterial and mammalian cells. This photo-controlled PAL-RNA interaction has been further used to reversibly regulate the cellular functions of micro RNAs and short hairpin RNAs in HEK293 cells. <sup>170</sup>

Our group have also recently demonstrated a genetically encoded RNA aptamer-based photosensitizer system, termed GRAP, for the targeted cell regulation in both prokaryotic and eukaryotic cells.<sup>171</sup> These photosensitizers can generate reactive oxygen species (ROS) upon light irradiation and lead to cell structure damages and photodynamic therapy. In this GRAP system, a DNB aptamer was used to selectively bind with a dinitroaniline quencher and separate it from the attached photosensitizer, which can further result in the restoration of the ROS generation (Fig. 9a). Meanwhile, the formation of the DNB aptamer structure could also be controlled by a target RNA of interest. This stimuli-responsive design has been validated in both *E. coli* and HeLa cells using different RNA targets (Fig. 9b). Wavelength-selective photosensitizing was also demonstrated in

this GRAP system. As shown by these initial examples, both reversible and irreversible photoregulated RNA nanodevices can be potentially used to precisely regulate cell functions.

## 5. Conclusions and future perspectives

In this review, we have discussed the current progress and milestones of using genetically encoded RNA-based nanodevices for intracellular gene regulation, fluorescence imaging, and other interesting applications. In this rapidly emerging and cutting-edge research area, numerous new design principles and functions have been shown recently. We hope the examples illustrated in this review will be helpful in inspiring further development of functional genetically encoded RNA nanodevices. In our own opinion, to allow these synthetic RNA devices to compete with, or to exceed, their protein or natural RNA rivals, there are still several important directions that need additional efforts and breakthroughs.

First of all, most of these synthetic RNA nanodevices have only been validated *in vitro* or in prokaryotic cells, like *E. coli*. Some of these studies are even limited in RNase-deficient *E. coli* strains. Indeed, expressing these RNA devices at a high level with reduced degradation is still a major challenge, especially in eukaryotic cells. Compared with proteins, normal cellular RNA concentrations are believed to be at least one magnitude lower. In nature, some RNA sequences can be partially protected based on different 5' and 3' structures and base modifications.<sup>172</sup> Inspired by these natural RNA protection mechanism, synthetic RNA nanodevices may also be similarly secured in the complex cellular environment. For example, a circular RNA expressing system has been designed by the Jaffrey group to significantly reduce the cellular degradation of synthetic RNA nanodevices.<sup>173</sup> While with the removal of both 5' and 3' ends, RNA devices have to be further carefully optimized in this circular RNA format. Other robust and reliable RNA expressing platform are still in great need for future eukaryotic and *in vivo* applications of synthetic RNA nanodevices.

Further advancement in programming algorithm is another critical direction to predict and guide the design of these RNA nanodevices. Even though a number of software such as Mfold<sup>28</sup> and NUPACK<sup>29</sup> have been successfully developed for the *in vitro* calculation and predication of the folding and assembly of nucleic acids. The cellular performance of RNA nanodevices in the events of cotranscriptional folding, target small molecule and protein binding, dynamic switching, and gene regulation is still very difficult to simulate. The dynamic nature and versatile interaction modes of these RNA structures have provided much freedom in designing sophisticated nanodevices. However, it also makes it hard to design and characterize these interactions, especially in the presence of other complicated cellular molecules and environment.

On the other hand, once we could computationally or experimentally understand the correlation between RNA sequences and their intracellular structures and dynamics, dramatic information on the cellular functions of natural non-coding RNAs could also be resulted from these advancements. These naturally existing functional RNA molecules can then further inspire new synthetic RNA nanodevices. Indeed, as mentioned above, riboswitches and ribozymes that discovered from bioinformatics analysis are important functional units now in building synthetic RNA nanodevices.

So far, natural RNA devices and structures are still way more complicated than the synthetic ones.

Such complicity may have resulted in the faster kinetics and larger dynamic range of these natural RNA nanodevices. Understanding the underlying mechanism of these precise and dynamic assemblies is important for the design of new RNA scaffolds in structural biology and for the construction of intelligent RNA network. To better interpret these design mechanism and increase the speed of developing functional RNA nanodevices, more reliable *in vitro* system to mimic intracellular environment, as well as high-throughput platform for the direct intracellular characterization, are highly demanded. With these further improvements, we believe, in the near future, genetically encoded RNA nanodevices will perform real intelligent intracellular diagnostics and therapeutics in a way, as good as, if not better than, their natural RNA and protein rivals.

#### **Conflicts of interest**

The authors declare no conflict of interest.

## Acknowledgements

The authors gratefully acknowledge the UMass Amherst start-up grant, NIH R01Al136789, NSF CAREER, and Alfred P. Sloan Research Fellowship to M. You. The authors also thank other members in the You Lab for useful discussion and valuable comments.

#### References

- 1 M. R. Jones, N. C. Seeman and C. A. Mirkin, *Science*, 2015, **347**, 1260901.
- 2 J. Li, L. Mo, C. H. Lu, T. Fu, H. H. Yang and W. Tan, *Chem. Soc. Rev.*, 2016, **45**, 1410–1431.
- 3 M. Xiao, W. Lai, T. Man, B. Chang, L. Li, A. R. Chandrasekaran and H. Pei, *Chem. Rev.*, 2019, **119**, 11631–11717.
- 4 L. A. Yatsunyk, O. Mendoza and J. L. Mergny, Acc. Chem. Res., 2014, 47, 1836–1844.
- W. Xu, W. He, Z. Du, L. Zhu, K. Huang, Y. Lu and Y. Luo, *Angew. Chem. Int. Ed.*, 2019, DOI: 10.1002/anie.201909927.
- 6 Y. Krishnan and N. C. Seeman, *Chem. Rev.*, 2019, **119**, 6271–6272.
- 7 M. S. Jani, A. T. Veetil and Y. Krishnan, *Nat. Rev. Mater.*, 2019, **4**, 451–458.
- 8 F. Pu, J. Ren and X. Qu, *Chem. Soc. Rev.*, 2018, **47**, 1285–1306.
- 9 Q. Hu, H. Li, L. Wang, H. Gu and C. Fan, *Chem. Rev.*, 2019, **119**, 6459–6506.
- 10 C. M. Platnich, F. J. Rizzuto, G. Cosa and H. F. Sleiman, *Chem. Soc. Rev.*, 2020, **49**, 4220–4233.
- 11 X. Wu, T. Wu, J. Liu and B. Ding, *Adv. Healthc. Mater.*, 2020, **9**, e2001046.
- 12 K. H. Leung, K. Chakraborty, A. Saminathan and Y. Krishnan, *Nat. Nanotechnol.*, 2019, **14**, 176–183.
- N. Narayanaswamy, K. Chakraborty, A. Saminathan, E. Zeichner, K. H. Leung, J. Devany and Y. Krishnan, *Nat. Methods*, 2019, **16**, 95–102.
- 14 M. S. Jani, J. Zou, A. T. Veetil and Y. Krishnan, *Nat. Chem. Biol.*, 2020, **16**, 660–666.
- 15 Z. Qing, J. Xu, J. Hu, J. Zheng, L. He, Z. Zou, S. Yang, W. Tan and R. Yang, *Angew. Chem. Int. Ed.*, 2019, **58**, 11574–11585.
- 16 J. Li, A. A. Green, H. Yan and C. Fan, *Nat. Chem.*, 2017, **9**, 1056–1067.
- 17 S. B. Ebrahimi, D. Samanta and C. A. Mirkin, *J. Am. Chem. Soc.*, 2020, **142**, 11343–11356.
- 18 A. Serganov and E. Nudler, *Cell*, 2013, **152**, 17–24.
- 19 M. C. Maurel, F. Leclerc and G. Hervé, Chem. Rev., 2020, 120, 4898–4918.

- L. R. Ganser, M. L. Kelly, D. Herschlag and H. M. Al-Hashimi, *Nat. Rev. Mol. Cell Biol.*, 2019,
  20, 474–489.
- 21 M. You and S. R. Jaffrey, Ann. N. Y. Acad. Sci., 2015, **1352**, 13–19.
- 22 M. Mandal and R. R. Breaker, *Nat. Rev. Mol. Cell Biol.*, 2004, **5**, 451–463.
- 23 J. Truong, Y. F. Hsieh, L. Truong, G. Jia and M. C. Hammond, *Methods*, 2018, **143**, 102–109.
- 24 K. Huang, F. Doyle, Z. E. Wurz, S. A. Tenenbaum, R. K. Hammond, J. L. Caplan and B. C. Meyers, *Nucleic Acids Res.*, 2017, **45**, e130.
- 25 Y. Su and M. C. Hammond, Curr. Opin. Biotechnol., 2020, **63**, 157–166.
- 26 F. J. Isaacs, D. J. Dwyer and J. J. Collins, *Nat. Biotechnol.*, 2006, **24**, 545–554.
- 27 T. R. Cech and J. A. Steitz, *Cell*, 2014, **157**, 77–94.
- 28 M. Zuker, *Nucleic Acids Res.*, 2003, **31**, 3406–3415.
- 29 B. R. Wolfe, N. J. Porubsky, J. N. Zadeh, R. M. Dirks and N. A. Pierce, *J. Am. Chem. Soc.*, 2017, **139**, 3134–3144.
- 30 P. E. M. Purnick and R. Weiss, *Nat. Rev. Mol. Cell Biol.*, 2009, **10**, 410–422.
- 31 M. Rossetti, E. Del Grosso, S. Ranallo, D. Mariottini, A. Idili, A. Bertucci and A. Porchetta, *Anal. Bioanal. Chem.*, 2019, **411**, 4293–4302.
- 32 J. C. Liang, R. J. Bloom and C. D. Smolke, *Mol. Cell*, 2011, **43**, 915–926.
- 33 L. S. Qi and A. P. Arkin, *Nat. Rev. Microbiol.*, 2014, **12**, 341–354.
- 34 M. McKeague, R. S. Wong and C. D. Smolke, *Nucleic Acids Res.*, 2016, **44**, 2987–2999.
- 35 Y. J. Lee and T. S. Moon, *Methods*, 2018, **143**, 58–69.
- 36 A. A. Green, *Emerg. Top. Life Sci.*, 2019, **3**, 507–516.
- 37 M. Kozak, *Gene*, 2005, **361**, 13–37.
- F. J. Isaacs, D. J. Dwyer, C. Ding, D. D. Pervouchine, C. R. Cantor and J. J. Collins, *Nat. Biotechnol.*, 2004, **22**, 841–847.
- 39 J. M. Callura, C. R. Cantor and J. J. Collins, *Proc. Natl. Acad. Sci. U. S. A.*, 2012, **109**, 5850–5855.
- 40 J. M. Callura, D. J. Dwyer, F. J. Isaacs, C. R. Cantor and J. J. Collins, *Proc. Natl. Acad. Sci. U. S. A.*, 2010, **107**, 15898–15903.
- 41 V. K. Mutalik, L. Qi, J. C. Guimaraes, J. B. Lucks and A. P. Arkin, *Nat. Chem. Biol.*, 2012, **8**, 447–454.
- 42 G. Rodrigo, T. E. Landrain and A. Jaramillo, *Proc. Natl. Acad. Sci. U. S. A.*, 2012, **109**, 15271–15276.
- 43 J. B. Lucks, L. Qi, V. K. Mutalik, D. Wang and A. P. Arkin, *Proc. Natl. Acad. Sci. U. S. A.*, 2011, **108**, 8617–8622.
- 44 M. K. Takahashi and J. B. Lucks, *Nucleic Acids Res.*, 2013, **41**, 7577–7588.
- 45 A. A. Green, P. A. Silver, J. J. Collins and P. Yin, *Cell*, 2014, **159**, 925–939.
- 46 K. Pardee, A. A. Green, T. Ferrante, D. E. Cameron, A. Daleykeyser, P. Yin and J. J. Collins, *Cell*, 2014, **159**, 940–954.
- 47 S. Wang, N. J. Emery and A. P. Liu, ACS Synth. Biol., 2019, 8, 1079–1088.
- 48 J. Chappell, M. K. Takahashi and J. B. Lucks, *Nat. Chem. Biol.*, 2015, **11**, 214–220.
- 49 C. C. Liu, L. Qi, J. B. Lucks, T. H. Segall-Shapiro, D. Wang, V. K. Mutalik and A. P. Arkin, *Nat. Methods*, 2012, **9**, 1088–1094.
- J. Chappell, A. Westbrook, M. Verosloff and J. B. Lucks, *Nat. Commun.*, 2017, **8**, 1051.
- 51 W. Winkler, A. Nahvi and R. R. Breaker, *Nature*, 2002, **419**, 952–956.
- A. S. Mironov, I. Gusarov, R. Rafikov, L. E. Lopez, K. Shatalin, R. A. Kreneva, D. A. Perumov and E. Nudler, *Cell*, 2002, **111**, 747–756.
- 53 A. Nahvi, N. Sudarsan, M. S. Ebert, X. Zou, K. L. Brown and R. R. Breaker, *Chem. Biol.*,

- 2002. **9**. 1043–1049.
- 54 G. A. Prody, J. T. Bakos, J. M. Buzayan, I. R. Schneider and G. Bruening, *Science*, 1986, **231**, 1577–1580.
- 55 A. C. Forster and R. H. Symons, *Cell*, 1987, **49**, 211–220.
- 56 W. C. Winkler and R. R. Breaker, *Annu. Rev. Microbiol.*, 2005, **59**, 487–517.
- 57 A. Serganov and D. J. Patel, *Nat. Rev. Genet.*, 2007, **8**, 776–790.
- 58 C. Tuerk and L. Gold, *Science*, 1990, **249**, 505–510.
- 59 A. D. Ellington and J. W. Szostak, *Nature*, 1990, **346**, 818–822.
- 60 G. Werstuck and M. R. Green, *Science*, 1998, **282**, 296–298.
- 61 S. Hanson, K. Berthelot, B. Fink, J. E. G. McCarthy and B. Suess, *Mol. Microbiol.*, 2003, **49**, 1627–1637.
- J. E. Weigand, M. Sanchez, E. B. Gunnesch, S. Zeiher, R. Schroeder and B. Suess, *RNA*, 2008, **14**, 89–97.
- 63 I. Harvey, P. Garneau and J. Pelletier, RNA, 2002, **8**, 452–463.
- 64 S. K. Desai and J. P. Gallivan, *J. Am. Chem. Soc.*, 2004, **126**, 13247–13254.
- 65 B. Suess, B. Fink, C. Berens, R. Stentz and W. Hillen, *Nucleic Acids Res.*, 2004, **32**, 1610–1614.
- 66 C. C. Fowler, E. D. Brown and Y. Li, *ChemBioChem*, 2008, **9**, 1906–1911.
- N. Dixon, J. N. Duncan, T. Geerlings, M. S. Dunstan, J. E. G. McCarthy, D. Leys and J. Micklefield, *Proc. Natl. Acad. Sci. U. S. A.*, 2010, **107**, 2830–2835.
- C. J. Robinson, H. A. Vincent, M. C. Wu, P. T. Lowe, M. S. Dunstan, D. Leys and J. Micklefield, *J. Am. Chem. Soc.*, 2014, **136**, 10615–10624.
- 69 M. C. Wu, P. T. Lowe, C. J. Robinson, H. A. Vincent, N. Dixon, J. Leigh and J. Micklefield, *J. Am. Chem. Soc.*, 2015, **137**, 9015–9021.
- A. Khvorova, A. Lescoute, E. Westhof and S. D. Jayasena, *Nat. Struct. Biol.*, 2003, **10**, 708–712.
- 71 M. Wieland, A. Benz, B. Klauser and J. S. Hartig, *Angew. Chem. Int. Ed.*, 2009, **48**, 2715–2718
- 72 K. M. Thompson, H. A. Syrett, S. M. Knudsen and A. D. Ellington, *BMC Biotechnol.*, 2002, **2**, 21.
- 73 N. W. Maung and C. D. Smolke, *Proc. Natl. Acad. Sci. U. S. A.*, 2007, **104**, 14283–14288.
- 74 M. Wieland and J. S. Hartig, *Angew. Chem. Int. Ed.*, 2008, **47**, 2604–2607.
- 75 A. Wittmann and B. Suess, *Mol. Biosyst.*, 2011, **7**, 2419–2427.
- M. Felletti, J. Stifel, L. A. Wurmthaler, S. Geiger and J. S. Hartig, *Nat. Commun.*, 2016, **7**, 12834.
- 77 M. Jinek, K. Chylinski, I. Fonfara, M. Hauer, J. A. Doudna and E. Charpentier, *Science*, 2012, **337**, 816–821.
- 78 G. J. Knott and J. A. Doudna, *Science*, 2018, **361**, 866–869.
- 79 M. Jinek, A. East, A. Cheng, S. Lin, E. Ma and J. Doudna, *Elife*, 2013, **2**, e00471.
- 80 W. Jiang, D. Bikard, D. Cox, F. Zhang and L. A. Marraffini, *Nat. Biotechnol.*, 2013, **31**, 233–239.
- 81 W. Y. Hwang, Y. Fu, D. Reyon, M. L. Maeder, S. Q. Tsai, J. D. Sander, R. T. Peterson, J. R. J. Yeh and J. K. Joung, *Nat. Biotechnol.*, 2013, **31**, 227–229.
- 82 S. W. Cho, S. Kim, J. M. Kim and J. S. Kim, *Nat. Biotechnol.*, 2013, **31**, 230–232.
- P. Mali, L. Yang, K. M. Esvelt, J. Aach, M. Guell, J. E. DiCarlo, J. E. Norville and G. M. Church, *Science*, 2013, **339**, 823–826.
- 84 L. Cong, F. A. Ran, D. Cox, S. Lin, R. Barretto, N. Habib, P. D. Hsu, X. Wu, W. Jiang, L. A.

- Marraffini and F. Zhang, Science, 2013, 339, 819-823.
- 85 L. S. Qi, M. H. Larson, L. A. Gilbert, J. A. Doudna, J. S. Weissman, A. P. Arkin and W. A. Lim, *Cell*, 2013, **152**, 1173–1183.
- 86 M. H. Larson, L. A. Gilbert, X. Wang, W. A. Lim, J. S. Weissman and L. S. Qi, *Nat. Protoc.*, 2013, **8**, 2180–2196.
- L. A. Gilbert, M. H. Larson, L. Morsut, Z. Liu, G. A. Brar, S. E. Torres, N. Stern-Ginossar, O. Brandman, E. H. Whitehead, J. A. Doudna, W. A. Lim, J. S. Weissman and L. S. Qi, *Cell*, 2013, **154**, 442.
- 88 Y. Liu, Y. Zhan, Z. Chen, A. He, J. Li, H. Wu, L. Liu, C. Zhuang, J. Lin, X. Guo, Q. Zhang, W. Huang and Z. Cai, *Nat. Methods*, 2016, **13**, 938–944.
- K. Kundert, J. E. Lucas, K. E. Watters, C. Fellmann, A. H. Ng, B. M. Heineike, C. M. Fitzsimmons, B. L. Oakes, J. Qu, N. Prasad, O. S. Rosenberg, D. F. Savage, H. El-Samad, J. A. Doudna and T. Kortemme, *Nat. Commun.*, 2019, **10**, 2127.
- 90 W. Tang, J. H. Hu and D. R. Liu, *Nat. Commun.*, 2017, **8**, 15939.
- 91 K. H. Siu and W. Chen, *Nat. Chem. Biol.*, 2019, **15**, 217–220.
- 92 M. H. Hanewich-Hollatz, Z. Chen, L. M. Hochrein, J. Huang and N. A. Pierce, *ACS Cent. Sci.*, 2019, **5**, 1241–1249.
- 93 K. Leung and Y. Krishnan, ACS Cent. Sci., 2019, **5**, 1111–1113.
- 94 Q. R. V. Ferry, R. Lyutova and T. A. Fulga, *Nat. Commun.*, 2017, **8**, 14633.
- 95 T. Péresse and A. Gautier, *Int. J. Mol. Sci.*, 2019, **20**, 6142.
- 96 J. Wu and S. R. Jaffrey, *Curr. Opin. Chem. Biol.*, 2020, **57**, 177–183.
- 97 E. C. Greenwald, S. Mehta and J. Zhang, *Chem. Rev.*, 2018, **118**, 11707–11794.
- 98 Z. Sun, T. Nguyen, K. McAuliffe and M. You, *Nanomaterials*, 2019, **9**, 233.
- 99 P. Swetha, Z. Fan, F. Wang and J. H. Jiang, *J. Mater. Chem. B*, 2020, **8**, 3382–3392.
- 100 A. F. L. Schneider and C. P. R. Hackenberger, Curr. Opin. Biotechnol., 2017, 48, 61–68.
- 101 F. Bouhedda, A. Autour and M. Ryckelynck, Int. J. Mol. Sci., 2018, 19, 44.
- 102 J. S. Paige, K. Y. Wu and S. R. Jaffrey, *Science*, 2011, **333**, 642–646.
- 103 G. S. Filonov, J. D. Moon, N. Svensen and S. R. Jaffrey, J. Am. Chem. Soc., 2014, 136, 16299–16308.
- 104 E. V. Dolgosheina, S. C. Y. Jeng, S. S. S. Panchapakesan, R. Cojocaru, P. S. K. Chen, P. D. Wilson, N. Hawkins, P. A. Wiggins and P. J. Unrau, *ACS Chem. Biol.*, 2014, **9**, 2412–2420.
- 105 W. Song, G. S. Filonov, H. Kim, M. Hirsch, X. Li, J. D. Moon and S. R. Jaffrey, *Nat. Chem. Biol.*, 2017, **13**, 1187–1194.
- 106 X. Chen, D. Zhang, N. Su, B. Bao, X. Xie, F. Zuo, L. Yang, H. Wang, L. Jiang, Q. Lin, M. Fang, N. Li, X. Hua, Z. Chen, C. Bao, J. Xu, W. Du, L. Zhang, Y. Zhao, L. Zhu, J. Loscalzo and Y. Yang, *Nat. Biotechnol.*, 2019, **37**, 1287–1293.
- 107 A. Arora, M. Sunbul and A. Jäschke, Nucleic Acids Res., 2015, 43, e144–e144.
- 108 M. Sunbul and A. Jäschke, *Angew. Chem. Int. Ed.*, 2013, **52**, 13401–13404.
- 109 R. L. Strack, M. D. Disney and S. R. Jaffrey, *Nat. Methods*, 2013, **10**, 1219–1224.
- 110 M. Okuda, D. Fourmy and S. Yoshizawa, *Nucleic Acids Res.*, 2017, **45**, 1404–1415.
- 111 A. D. Cawte, P. J. Unrau and D. S. Rueda, Nat. Commun., 2020, 11, 1283.
- 112 E. Braselmann, T. Stasevich, K. Lyon, R. Batey and A. Palmer, *bioRxiv*, 2019, DOI:10.1101/701649.
- 113 X. Li, H. Kim, J. L. Litke, J. Wu and S. R. Jaffrey, *Angew. Chem. Int. Ed.*, 2020, **59**, 4511–4518.
- 114 J. Wu, S. Zaccara, D. Khuperkar, H. Kim, M. E. Tanenbaum and S. R. Jaffrey, *Nat. Methods*, 2019, **16**, 862–865.

- 115 Z. Wang, Y. Luo, X. Xie, X. Hu, H. Song, Y. Zhao, J. Shi, L. Wang, G. Glinsky, N. Chen, R. Lal and C. Fan, *Angew. Chem. Int. Ed.*, 2018, **57**, 972–976.
- 116 K. K. Alam, K. D. Tawiah, M. F. Lichte, D. Porciani and D. H. Burke, *ACS Synth. Biol.*, 2017,6, 1710–1721.
- 117 A. P. K. K. Karunanayake Mudiyanselage, Q. Yu, M. A. Leon-Duque, B. Zhao, R. Wu and M. You, *J. Am. Chem. Soc.*, 2018, **140**, 8739–8745.
- 118 C. Wu, S. Cansiz, L. Zhang, I. T. Teng, L. Qiu, J. Li, Y. Liu, C. Zhou, R. Hu, T. Zhang, C. Cui, L. Cui and W. Tan, *J. Am. Chem. Soc.*, 2015, **137**, 4900–4903.
- 119 P. Yin, H. M. T. Choi, C. R. Calvert and N. A. Pierce, *Nature*, 2008, **451**, 318–322.
- 120 K. Ren, R. Wu, A. P. K. K. Karunanayake Mudiyanselage, Q. Yu, B. Zhao, Y. Xie, Y. Bagheri, Q. Tian and M. You, *J. Am. Chem. Soc.*, 2020, **142**, 2968–2974.
- 121 J. S. Paige, T. Nguyen-Duc, W. Song and S. R. Jaffrey, *Science*, 2012, **335**, 1194.
- 122 C. A. Kellenberger, C. Chen, A. T. Whiteley, D. A. Portnoy and M. C. Hammond, *J. Am. Chem. Soc.*, 2015, **137**, 6432–6435.
- 123 C. A. Kellenberger, S. C. Wilson, J. Sales-Lee and M. C. Hammond, *J. Am. Chem. Soc.*, 2013, **135**, 4906–4909.
- 124 W. Song, R. L. Strack and S. R. Jaffrey, *Nat. Methods*, 2013, **10**, 873–875.
- 125 E. B. Porter, J. T. Polaski, M. M. Morck and R. T. Batey, *Nat. Chem. Biol.*, 2017, **13**, 295–301.
- 126 X. Li, L. Mo, J. L. Litke, S. K. Dey, S. R. Suter and S. R. Jaffrey, *J. Am. Chem. Soc.*, 2020, **142**, 14117–14124.
- 127 R. Wu, A. P. K. K. Karunanayake Mudiyanselage, F. Shafiei, B. Zhao, Y. Bagheri, Q. Yu, K. McAuliffe, K. Ren and M. You, *Angew. Chem. Int. Ed.*, 2019, **58**, 18271–18275.
- 128 R. Wu, A. P. K. K. Karunanayake Mudiyanselage, K. Ren, Z. Sun, Q. Tian, B. Zhao, Y. Bagheri, D. Lutati, P. Keshri and M. You, *ACS Appl. Bio Mater.*, 2020, **3**, 2633–2642.
- 129 A. S. V. Bédard, E. D. M. Hien and D. A. Lafontaine, *Biochim. Biophys. Acta Gene Regul. Mech.*, 2020, **1863**, 194501.
- 130 M. You, J. L. Litke and S. R. Jaffrey, *Proc. Natl. Acad. Sci. U. S. A.*, 2015, **112**, E2756–E2765.
- 131 L. Ma and J. Liu, *iScience*, 2020, **23**, 100815.
- 132 S. V. Park, J. S. Yang, H. Jo, B. Kang, S. S. Oh and G. Y. Jung, *Biotechnol. Adv.*, 2019, **37**, 107452.
- 133 R. Penchovsky, *Biotechnol. Adv.*, 2014, **32**, 1015–1027.
- 134 J. Frommer, B. Appel and S. Müller, Curr. Opin. Biotechnol., 2015, 31, 35–41.
- 135 V. Scognamiglio, A. Antonacci, M. D. Lambreva, S. C. Litescu and G. Rea, *Biosens. Bioelectron.*, 2015, **74**, 1076–1086.
- 136 M. You, J. L. Litke, R. Wu and S. R. Jaffrey, Cell Chem. Biol., 2019, 26, 471-481.e3.
- 137 E. A. Jares-Erijman and T. M. Jovin, *Nat. Biotechnol.*, 2003, **21**, 1387–1395.
- Y. L. Chiu, S. A. Chen, J. H. Chen, K. J. Chen, H. L. Chen and H. W. Sung, *ACS Nano*, 2010,4, 7467–7474.
- 139 L. Wu, C. Huang, B. P. Emery, A. C. Sedgwick, S. D. Bull, X. P. He, H. Tian, J. Yoon, J. L. Sessler and T. D. James, *Chem. Soc. Rev.*, 2020, 49, 5110–5139.
- 140 J. Molle, L. Jakob, J. Bohlen, M. Raab, P. Tinnefeld and D. Grohmann, *Nanoscale*, 2018, **10**, 16416–16424.
- 141 K. Quan, C. Yi, X. Yang, X. He, J. Huang and K. Wang, *TrAC Trends Anal. Chem.*, 2020, **124**, 115784.
- 142 H. Ohno, S. Akamine and H. Saito, *Curr. Opin. Biotechnol.*, 2019, **58**, 53–61.

- T. Shibata, Y. Fujita, H. Ohno, Y. Suzuki, K. Hayashi, K. R. Komatsu, S. Kawasaki, K. Hidaka, S. Yonehara, H. Sugiyama, M. Endo and H. Saito, *Nat. Commun.*, 2017, **8**, 540.
- 144 M. D. E. Jepsen, S. M. Sparvath, T. B. Nielsen, A. H. Langvad, G. Grossi, K. V. Gothelf and E. S. Andersen, *Nat. Commun.*, 2018, **9**, 18.
- 145 R. S. Braich, N. Chelyapov, C. Johnson, P. W. K. Rothemund and L. Adleman, *Science*, 2002, **296**, 499–502.
- J. Elbaz, O. Lioubashevski, F. Wang, F. Remacle, R. D. Levine and I. Willner, *Nat. Nanotechnol.*, 2010, **5**, 417–422.
- 147 L. Qian, E. Winfree and J. Bruck, *Nature*, 2011, **475**, 368–372.
- 148 Y. J. Chen, B. Groves, R. A. Muscat and G. Seelig, *Nat. Nanotechnol.*, 2015, **10**, 748–760.
- 149 Y. Benenson, Curr. Opin. Biotechnol., 2009, 20, 471–478.
- 150 V. Sharma, Y. Nomura and Y. Yokobayashi, *J. Am. Chem. Soc.*, 2008, **130**, 16310–16315.
- 151 N. W. Maung and C. D. Smolke, *Science*, 2008, **322**, 456–460.
- 152 A. A. Green, J. Kim, D. Ma, P. A. Silver, J. J. Collins and P. Yin, *Nature*, 2017, **548**, 117–121.
- J. Kim, Y. Zhou, P. D. Carlson, M. Teichmann, S. Chaudhary, F. C. Simmel, P. A. Silver, J. J. Collins, J. B. Lucks, P. Yin and A. A. Green, *Nat. Chem. Biol.*, 2019, **15**, 1173–1182.
- N. D. Derr, B. S. Goodman, R. Jungmann, A. E. Leschziner, W. M. Shih and S. L. Reck-Peterson, *Science*, 2012, **338**, 662–665.
- J. Fu, Y. R. Yang, A. Johnson-Buck, M. Liu, Y. Liu, N. G. Walter, N. W. Woodbury and H. Yan, *Nat. Nanotechnol.*, 2014, **9**, 531–536.
- 156 W. M. Shih, J. D. Quispe and G. F. Joyce, *Nature*, 2004, **427**, 618–621.
- 157 P. W. K. Rothemund, *Nature*, 2006, **440**, 297–302.
- 158 C. Lin, S. Rinker, X. Wang, Y. Liu, N. C. Seeman and H. Yan, *Proc. Natl. Acad. Sci. U. S. A.*, 2008, **105**, 17626–17631.
- 159 C. Ducani, C. Kaul, M. Moche, W. M. Shih and B. Högberg, *Nat. Methods*, 2013, **10**, 647–652.
- 160 J. Elbaz, P. Yin and C. A. Voigt, *Nat. Commun.*, 2016, **7**, 11179.
- F. Praetorius, B. Kick, K. L. Behler, M. N. Honemann, D. Weuster-Botz and H. Dietz, *Nature*, 2017, **552**, 84–87.
- D. Han, X. Qi, C. Myhrvold, B. Wang, M. Dai, S. Jiang, M. Bates, Y. Liu, B. An, F. Zhang, H. Yan and P. Yin, *Science*, 2017, **358**, eaao2648.
- 163 C. J. Delebecque, A. B. Lindner, P. A. Silver and F. A. Aldaye, *Science*, 2011, **333**, 470–474.
- 164 K. A. Afonin, W. W. Grabow, F. M. Walker, E. Bindewald, M. A. Dobrovolskaia, B. A. Shapiro and L. Jaeger, *Nat. Protoc.*, 2011, **6**, 2022–2034.
- 165 C. Geary, P. W. K. Rothemund and E. S. Andersen, *Science*, 2014, **345**, 799–804.
- 166 M. Li, M. Zheng, S. Wu, C. Tian, D. Liu, Y. Weizmann, W. Jiang, G. Wang and C. Mao, *Nat. Commun.*, 2018, 9, 2196.
- 167 D. D. Young and A. Deiters, *ChemBioChem*, 2008, **9**, 1225–1228.
- 168 G. Hayashi, M. Hagihara and K. Nakatani, *Chem. A Eur. J.*, 2009, **15**, 424–432.
- A. M. Weber, J. Kaiser, T. Ziegler, S. Pilsl, C. Renzl, L. Sixt, G. Pietruschka, S. Moniot, A. Kakoti, M. Juraschitz, S. Schrottke, L. Lledo Bryant, C. Steegborn, R. Bittl, G. Mayer and A. Möglich, *Nat. Chem. Biol.*, 2019, **15**, 1085–1092.
- 170 S. Pilsl, C. Morgan, M. Choukeife, A. Möglich and G. Mayer, Nat. Commun., 2020, 11, 4825.
- 171 K. Ren, P. Keshri, R. Wu, Z. Sun, Q. Yu, Q. Tian, B. Zhao, Y. Bagheri, Y. Xie and M. You, *Angew. Chem. Int. Ed.*, 2020, **59**, 21986–21990.
- 172 J. Houseley and D. Tollervey, *Cell*, 2009, **136**, 763–776.
- 173 J. L. Litke and S. R. Jaffrey, *Nat. Biotechnol.*, 2019, **37**, 667–675.

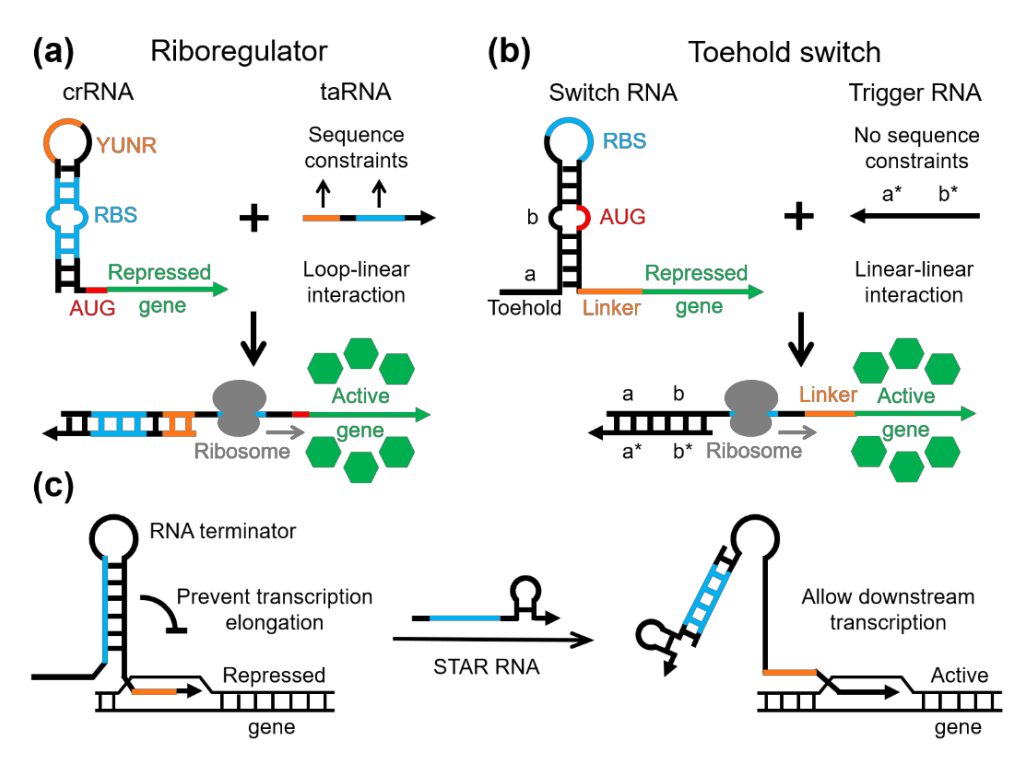
- W. Song, R. L. Strack, N. Svensen and S. R. Jaffrey, J. Am. Chem. Soc., 2014, 136, 1198– 1201.
- 175 H. Guo, M. Fan, Z. Li, W. Tang and X. Duan, *Anal. Methods*, 2018, **10**, 5629–5633.
- 176 A. Autour, S. C. Y. Jeng, A. D. Cawte, A. Abdolahzadeh, A. Galli, S. S. S. Panchapakesan, D. Rueda, M. Ryckelynck and P. J. Unrau, *Nat. Commun.*, 2018, **9**, 656.
- 177 X. Tan, T. P. Constantin, K. L. Sloane, A. S. Waggoner, M. P. Bruchez and B. A. Armitage, *J. Am. Chem. Soc.*, 2017, **139**, 9001–9009.
- 178 C. Steinmetzger, N. Palanisamy, K. R. Gore and C. Höbartner, *Chem. A Eur. J.*, 2019, **25**, 1931–1935.
- 179 R. Wirth, P. Gao, G. U. Nienhaus, M. Sunbul and A. Jäschke, *J. Am. Chem. Soc.*, 2019, **141**, 7562–7571.
- F. Bouhedda, K. T. Fam, M. Collot, A. Autour, S. Marzi, A. Klymchenko and M. Ryckelynck, *Nat. Chem. Biol.*, 2020, **16**, 69–76.
- M. Sunbul, J. Lackner, A. Martin, D. Englert, B. Hacene, F. Grun, K. Nienhaus, G. U. Nienhaus and A. Jäschke, *Nat. Biotechnol.*, 2021, DOI: 10.1038/s41587-020-00794-3.
- 182 A. Murata, S. Ichi Sato, Y. Kawazoe and M. Uesugi, *Chem. Commun.*, 2011, **47**, 4712–4714.

Table 1 Spectral and biophysical characteristics of commonly used fluorogenic RNA aptamers

RNA aptamer	Fluorophore	K <sub>D</sub>	E <sub>x</sub> /E <sub>m</sub>	ε (M <sup>-1</sup>	φ	Length	Ref.
•	•	(nM)	(nm)	cm <sup>-1</sup> )	•	(nt)	
Spinach	DFHBI	540	469/501	24,300	0.72	98	102
Spinach2	DFHBI-1T	560	482/505	31000	0.94	95	174
Spinach2	DFHBI	530	447/501	22000	0.72	95	174
Spinach2	DFHBI-2T	1300	500/523	29000	0.12	95	174
Spinach2	DFHBI-CM	N/A	447/502	N/A	N/A	95	175
Broccoli	DFHBI-1T	360	472/507	29600	0.94	49	103
Broccoli	BI	51	470/505	33600	0.67	49	113
Red Broccoli	DFHO	206	518/582	35000	0.34	49	105
Orange Broccoli	DFHO	230	513/562	34000	0.28	49	105
Red Broccoli	OBI	23	541/590	47300	0.67	54	126
Corn	DFHO	70	505/545	29000	0.25	36	105
Mango	TO1-Biotin	3.6	510/535	77500	0.16	29	104
Mango II	TO1-Biotin	0.7	510/535	77000	0.2	29	176
Mango III	TO1-Biotin	5.6	510/535	77000	0.56	29	176
Mango IV	TO1-Biotin	11.1	510/535	77000	0.42	29	176
DIR2s-Apt	DIR-pro	252	600/658	164000	0.33	57	177
DIR2s-Apt	OTB-SO3	662	380/421	73000	0.51	57	177
Chili	DMHBI <sup>+</sup>	63	413/542	21000	0.4	52	178
Chili	DMHBO <sup>+</sup>	12	456/592	22000	0.1	52	178
SiRA	SiR	430	649/662	86000	0.98	46	179
Pepper485	HBC485	8	443/485	49100	0.42	43	106
Pepper497	HBC497	6.7	435/497	54700	0.57	43	106
Pepper508	HBC508	27	458/508	42500	0.3	43	106
Pepper514	HBC514	12	458/514	44100	0.45	43	106
Pepper525	HBC525	3.8	491/525	74100	0.7	43	106
Pepper530	HBC530	3.5	485/530	65300	0.66	43	106
Pepper599	HBC599	18	515/599	54400	0.43	43	106
Pepper620	HBC620	6.1	577/620	100000	0.58	43	106
SRB-2	SR-DN	1400	579/596	N/A	0.65	54	108
o-Coral	Gemini-561	73	580/596	141000	0.58	150	180
RhoBAST	TMR-DN	15	564/590	96000	0.57	55	181
DNB	TMR-DN	350	555/582	47150	0.9	75	107
DNB	SR-DN	800	572/591	50250	0.98	75	107
BHQ apt (A1)	Cy3-BHQ1	4700	520/565	N/A	N/A	60	182

N/A, not available;  $\quad \epsilon,$  absorption coefficient;  $\ \varphi,$  quantum yield;

 $E_{\mbox{\tiny X}}/E_{\mbox{\tiny m}},$  excitation/emission wavelength peak value.



**Fig. 1** (a) Schematic of a riboregulator-based RNA nanodevice for the translation control. The binding of a *trans*-activating RNA (taRNA) with a *cis*-repressed mRNA (crRNA) exposes the ribosome binding site (RBS) and results in a translation initiation.<sup>38</sup> (b) Schematic of a toehold switch-based RNA nanodevice for the translation control. The use of an unpaired RBS and AUG region removes the sequence constrains in the conventional riboregulator design. The binding of a trigger RNA with a switch RNA leads to protein translation.<sup>45</sup> (c) Schematic of STAR-based RNA nanodevice for the transcription control. The binding of a STAR RNA to the terminator sequence promotes the downstream transcription elongation.<sup>48</sup>

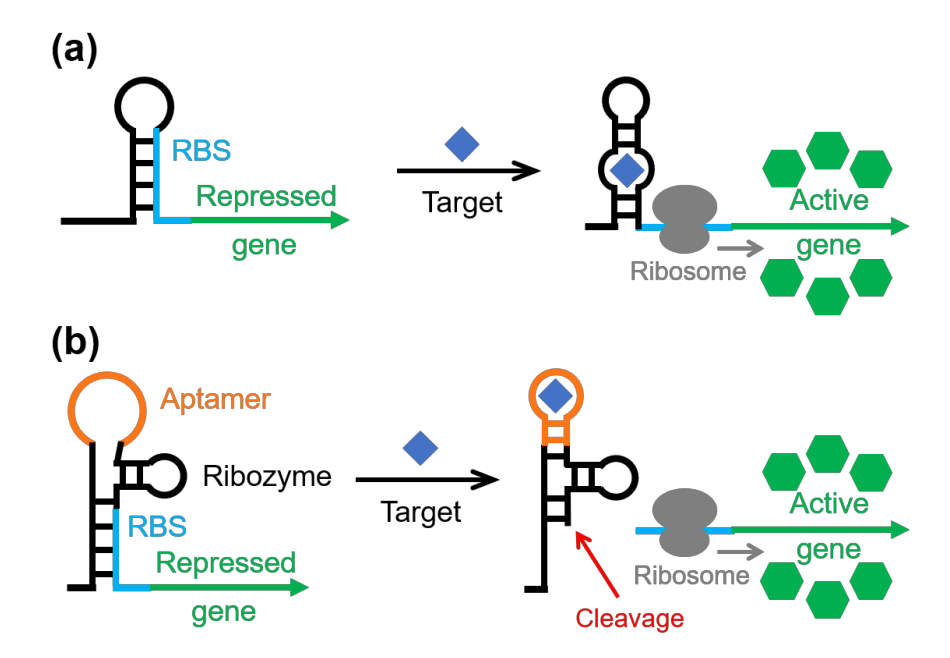


**Fig. 2** (a) Schematic of a riboswitch-based RNA nanodevice for the gene regulation during prokaryotic protein synthesis. The binding of a target ligand induces the RNA conformational change, exposes the ribosome binding site (RBS) for the protein synthesis. (b) Schematic of a hammerhead ribozyme-based RNA nanodevice for the gene regulation. The binding of a target ligand induces the folding and catalytic function of the hammerhead ribozyme. As a result, the RBS region is released and exposed to start the protein synthesis.

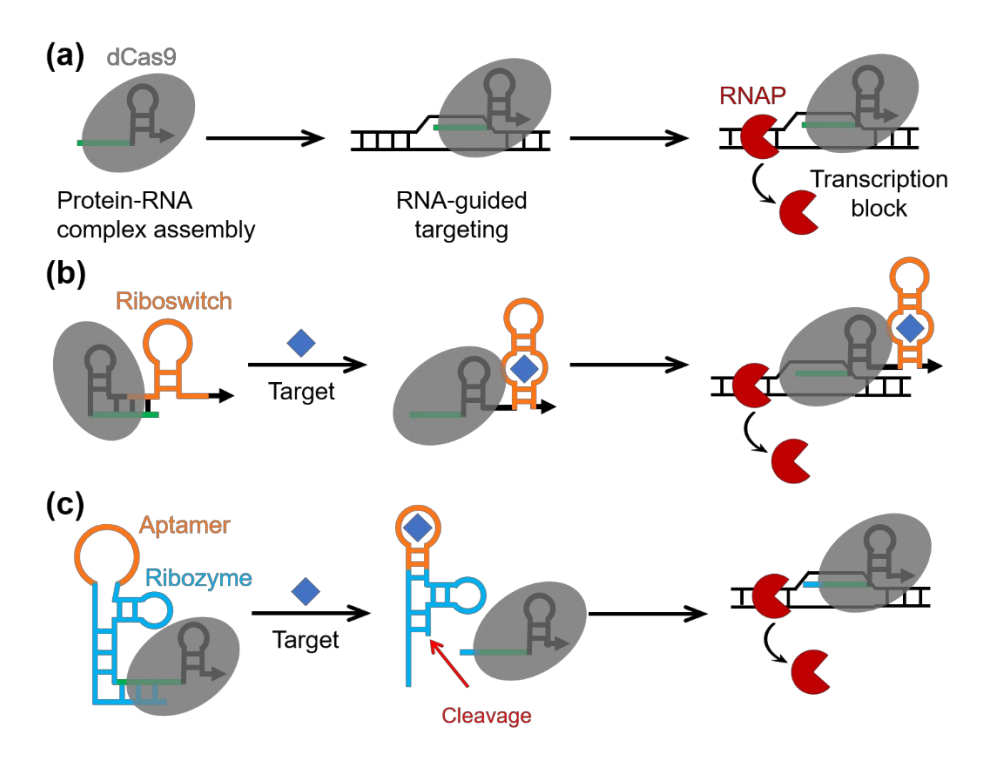


**Fig. 3** (a) Schematic of a CRISPR interference (CRISPRi) system for the gene regulation. A dead Cas9 (dCas9) protein binds to a single guide RNA (sgRNA) and facilitates its association with the target gene. The association of the dCas9/sgRNA complex further sterically blocks the transcription function of the RNA polymerase (RNAP).<sup>85</sup> (b) Schematic of a target-inducible CRISPRi system. A target-binding aptamer is designed to partially hybridize with the sgRNA. The binding of the target ligand refolds the aptamer and releases the sgRNA to activate gene regulation.<sup>88</sup> (c) Schematic of an aptazyme-regulated CRISPRi system. The binding of the target ligand induces the cleavage of the ribozyme and releases the sgRNA, which results in a target-controlled gene regulation.<sup>90</sup>

**Fig. 4** Chemical structures of commonly used chromophores that can be recognized and activated by RNA aptamers. The corresponding fluorogenic RNA aptamer for each chromophore has been listed in Table 1.

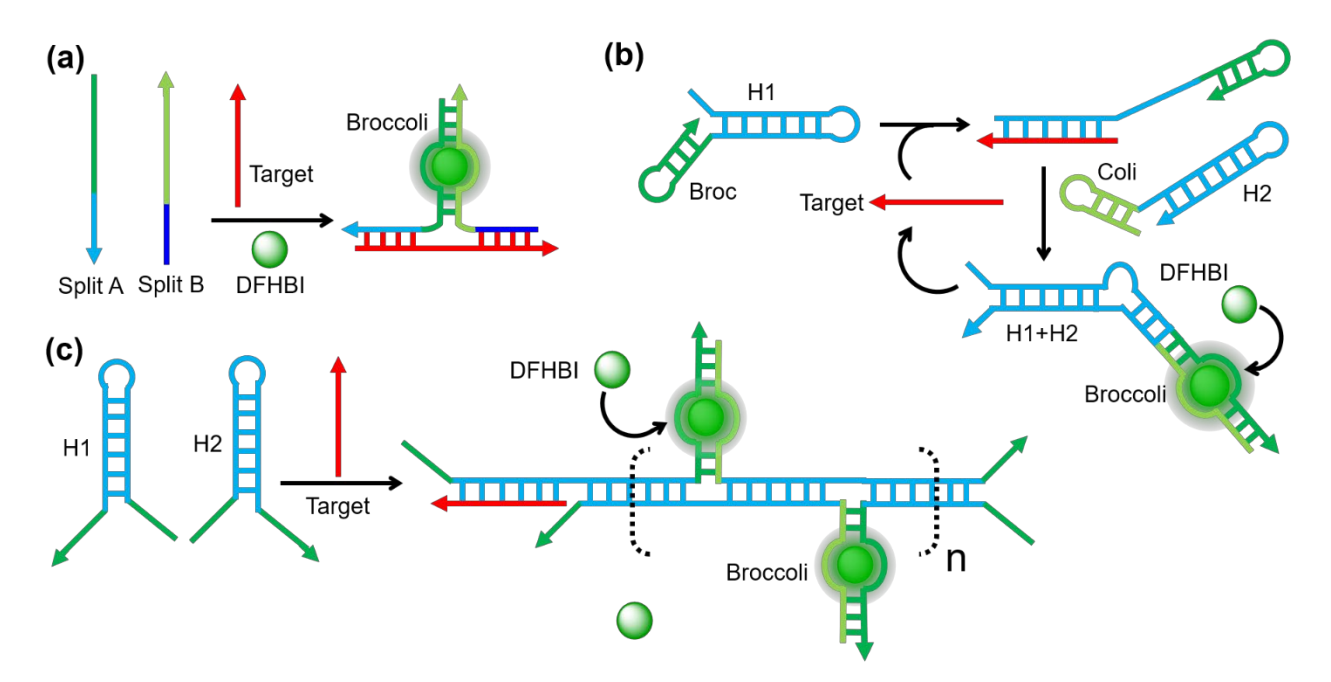


**Fig. 5** (a) Schematics of a split Broccoli-based nanodevice for imaging target RNAs. The binding of the target RNA to both split fragments of Broccoli reassembles the DFHBI-binding pocket and activates the fluorescence. (b) Schematic of a CHARGE circuit. Two Broccoli fragments are respectively conjugated to the terminal of a hairpin pair, H1 and H2. The binding of a target RNA triggers a catalytic hairpin assembly reaction between H1 and H2, generates multiple Broccoli aptamers and activates an amplified signal. (c) Schematic of an INSIGHT nanodevice. The binding of a target RNA initiates a cascaded H1/H2 hybridization chain reaction and assembles a Broccoli aptamer chain for cellular tracking of the target location.

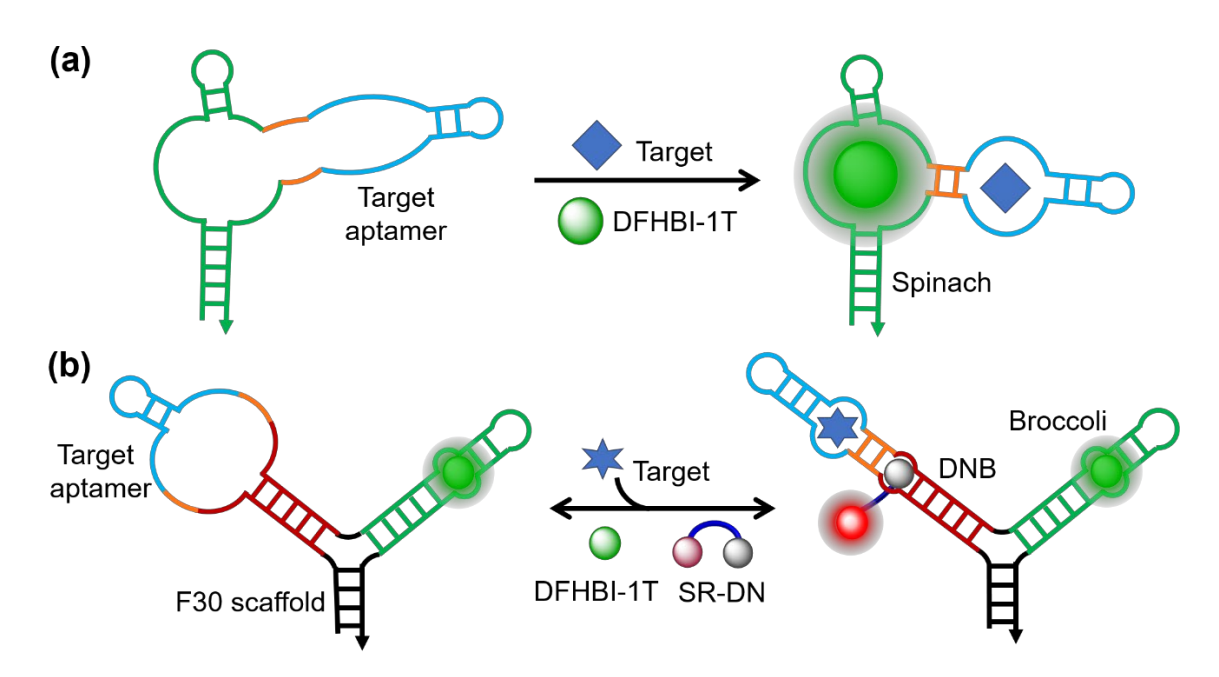


**Fig. 6** (a) Schematic of an allosteric Spinach-based nanodevice for cellular imaging. The binding of the target molecule stabilizes the transducer (orange) and facilitates the formation of Spinach to activate the DFHBI fluorescence. (b) Schematic of a ratiometric fluorogenic RNA device including an F30 scaffold (black), Broccoli (green), DNB (red) and target-binding aptamer (blue). The binding of the target induces the folding of DNB and activates the SR-DN fluorescence. A DNB-to-Broccoli ratiometric fluorescence signal is used to quantify the cellular concentrations of the target. 127

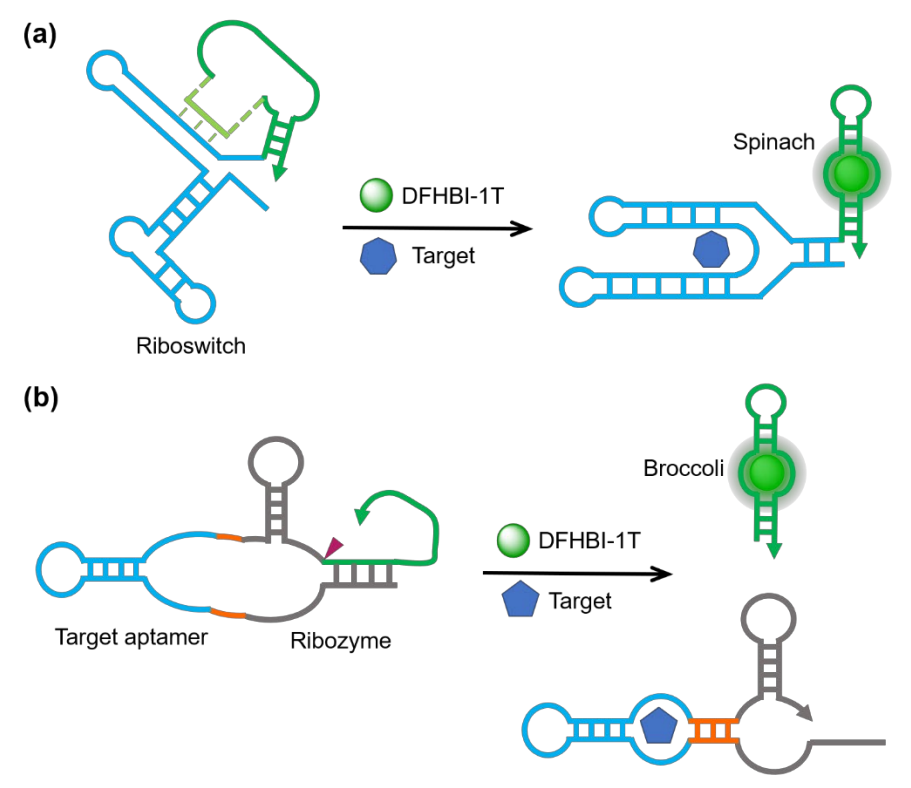


**Fig. 7** (a) Schematic of a Spinach riboswitch-based nanodevice for cellular imaging. The binding of the target induces the release of a transducer sequence (light green) from the switching sequence (red) and reassembles the Spinach aptamer for the fluorescence activation. (b) Schematic of an allosteric ribozyme-based nanodevice. The binding of the target induces the cleavage of the ribozyme and releases the Broccoli aptamer to activate the DFHBI-1T fluorescence signal. 136

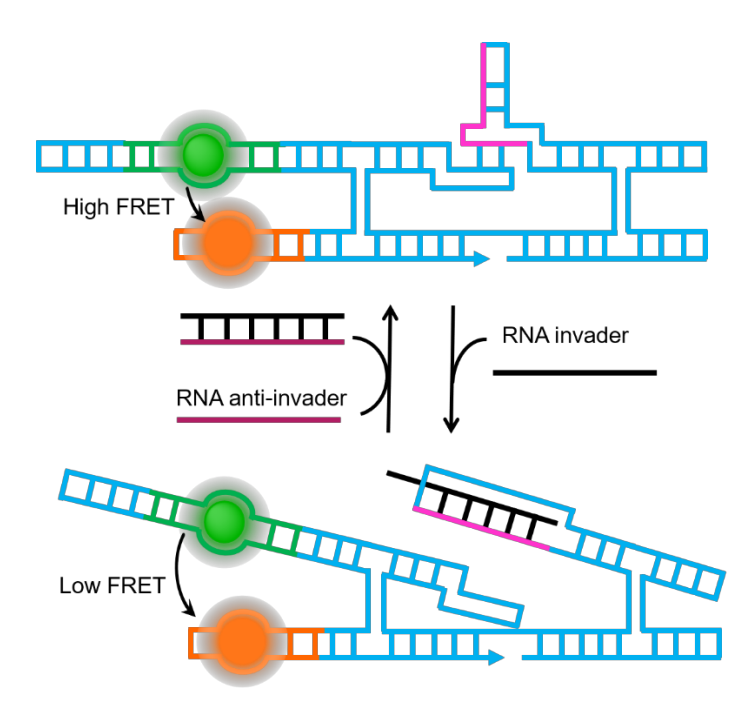


**Fig. 8** Schematic of an RNA origami-based fluorogenic RNA FRET nanodevice. The binding of the target RNA induces the conformational transformation of the origami, changes the distance between a fluorogenic RNA FRET pair and the corresponding fluorescence signal.<sup>144</sup>

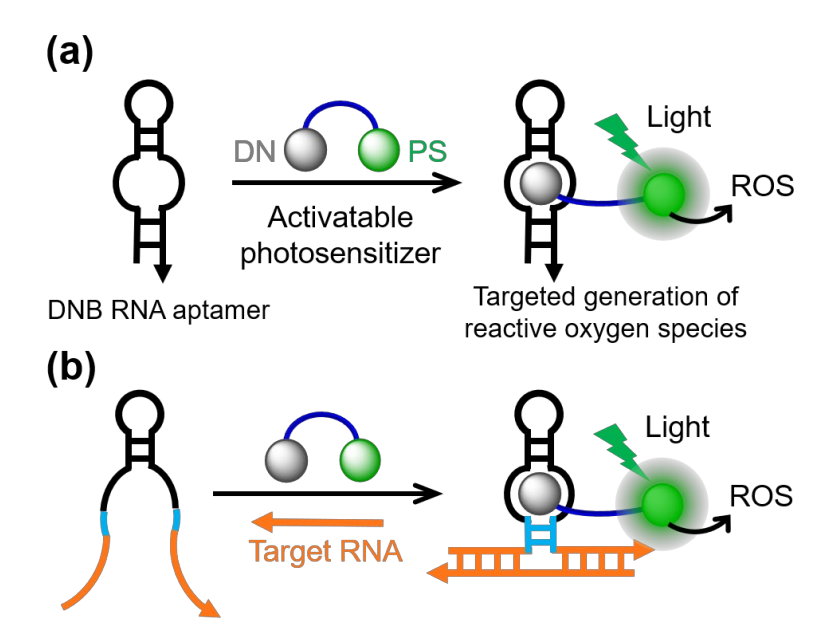


**Fig. 9** (a) Schematic of an RNA aptamer-activated photosensitizer. A photosensitizer (PS) is originally quenched by the attached dinitroaniline (DN) quencher. The binding of a DNB aptamer with the DN quencher can restore the PS to generate reactive oxygen species (ROS) upon light irradiation. (b) Schematic of a target-activated photosensitizer RNA nanodevice. The addition of a target RNA refolds the DNB aptamer, which can further lead to the reactivation of the PS. 171 Schematic of a target-activated photosensitizer RNA nanodevice. 171